Ecological Modelling 510 (2025) 111337

Contents lists available at ScienceDirect

Ecological Modelling

journal homepage: www.elsevier.com/locate/ecolmodel

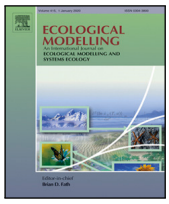

Spatial variability in defoliation dynamics during spruce budworm outbreaks: A landscape perspective

Olaloudé Judicaël Franck Osse [a,b,c,*], Philippe Marchand [b], Miguel Montoro Girona [a,b,c,d]

[a] Centre d'Étude de la Forêt, Institut de Recherche sur les Forêts (CEF-IRF), Université du Québec en Abitibi-Témiscamingue, 445 boulevard de l'Université, Rouyn-Noranda, Québec, Canada
[b] Chaire UQAT-UQAM en Aménagement Forestier Durable, 445 boulevard de l'Université, Rouyn-Noranda, Québec, Canada
[c] Groupe de Recherche en Écologie de la MRC Abitibi (GREMA), Forest Research Institute, Université du Québec en Abitibi-Témiscamingue, 341 Rue Principale Nord, Amos, Québec, J9T 2L8, Canada
[d] Grupo de Análisis y Planificación del Medio Natural, Universidad de Huelva, Avda. Fuerzas Armadas, Huelva, 21001, Spain

ARTICLE INFO

Keywords:
Climate
Defoliation
Clustering
Forest disturbances
Ecological modeling
Adjacent-category autoregressive model

ABSTRACT

Our study explored the spatiotemporal dynamics of spruce budworm (SBW) defoliation in Quebec's boreal forests, highlighting how climatic factors, historical defoliation, and landscape heterogeneity intersect. SBW outbreaks are a major disturbance in these ecosystems, with significant ecological and economic repercussions—underscoring the need to understand the mechanisms that drive them. Although previous research has linked warming temperatures and past defoliation patterns to more severe outbreaks, their localized effects remain poorly characterized. Our aim is to clarify these localized processes and support more targeted forest management strategies.

We employed an adjacent-category autoregressive (ACAR) model specifically designed for ordinal defoliation data spanning 1992–2022. Defoliation was categorized into three severity levels: none, light, and moderate/severe. Key climate variables — most notably spring and summer temperatures, as well as precipitation — were obtained from BioSIM and assigned to each landscape unit (LU). After fitting individual ACAR models to each LU and confirming their adequacy via the Portmanteau test, we identified the best models using the Akaike Information Criterion (AIC). A clustering analysis then grouped LUs with comparable model parameters into distinct ecological response clusters.

Our findings reveal that temperature exerts a non-linear influence on SBW defoliation: while warmer spring and summer conditions can initially facilitate larval survival, exceedingly high temperatures reduce defoliation by surpassing larval thermal tolerance and disrupting phenological synchrony with host trees. Additionally, strong autoregressive feedback values (β_1, β_2) underscore the cumulative effect of past defoliation—trees weakened by previous outbreaks become more susceptible to subsequent infestations, triggering feedback loops that endanger long-term forest health. Through clustering, we identified five distinct landscape groups. The more homogeneous clusters (Clusters 4 and 5) displayed either relatively stable precipitation patterns or pronounced temperature variability, each with high silhouette scores (0.55 and 0.24, respectively), indicating clear opportunities for targeted management. Meanwhile, heterogeneous clusters like Cluster 1 (silhouette score: −0.43) exhibited overlapping characteristics that warrant further investigation.

Overall, these results emphasize the importance of localized management approaches that account for climatic thresholds and historical defoliation patterns. Pinpointing temperature extremes and incorporating the impacts of cumulative defoliation can guide both the timing and intensity of interventions. Future research may integrate additional spatial factors, such as forest composition and connectivity, to refine outbreak predictions further. Ultimately, adaptive, multi-scale management is essential for maintaining the resilience of boreal forests in a changing climate.

* Corresponding author at: Centre d'Étude de la Forêt, Institut de Recherche sur les Forêts (CEF-IRF), Université du Québec en Abitibi-Témiscamingue, 445 boulevard de l'Université, Rouyn-Noranda, Québec, Canada.
E-mail address: olaloudejudicaelfranck.osse@uqat.ca (O.J.F. Osse).

https://doi.org/10.1016/j.ecolmodel.2025.111337
Received 6 June 2025; Received in revised form 20 August 2025; Accepted 30 August 2025
Available online 11 September 2025

1. Introduction

The boreal forest, which extends across vast regions of North America, is a complex ecosystem that supports a wide range of plant, animal, and microbial life (Hansen et al., 2010; Brockerhoff et al., 2017). This biome plays an essential role in global carbon storage and climate regulation, making it a crucial element in the ecological balance of the Earth (Pan et al., 2011; Xu and Hisano, 2024; Gauthier et al., 2023). However, the boreal forest is particularly vulnerable to natural and anthropogenic disturbances (Frelich et al., 2024; Seidl et al., 2020, 2023). One of the most significant threats is the periodic outbreak of the spruce budworm (*Choristoneura fumiferana* Clem.), a native insect that specifically targets coniferous trees (Sidhu et al., 2024). Recurring every 30 to 40 years, SBW outbreaks involve massive larval populations that feed on host tree foliage of host trees. During these infestations, trees suffer extensive defoliation, which not only weakens their overall health but also compromises their growth and resilience (Debaly et al., 2022; Doran et al., 2017). Extending our earlier work on the adjacent-category autoregressive (ACAR) model (Osse et al., 2023), we now delve deeper into how spatial heterogeneity influences SBW defoliation dynamics across the boreal landscape. When defoliation persists for multiple years (on average five), tree mortality rates can become alarmingly high (Houndode et al., 2021; Fierravanti et al., 2019; MacLean et al., 2024), especially in stands dominated by balsam fir (*Abies balsamea*) and white spruce (*Picea glauca*) (Lemay et al., 2022; Kneeshaw et al., 2022). Despite ongoing research on the ecological and economic consequences of SBW outbreaks, the boreal forest's vulnerability is compounded by its limited ability to recover quickly under increasingly variable climatic conditions (Seidl et al., 2017).

Although numerous studies have already demonstrated the critical influence of temperature, precipitation, and landscape factors on the severity of SBW outbreaks (Li et al., 2020; Régnière and Nealis, 2019; Subedi et al., 2023; Bouchard and Auger, 2014; Bouchard et al., 2018; Fierravanti et al., 2015), the methods commonly used to model their effects on outbreak development present several limitations. On the one hand, most current approaches focus on the broad-scale effects of climate (Gray, 2013; Navarro et al., 2018; Bouchard et al., 2018), often neglecting the fine-scale integration of spatiotemporal heterogeneity in models. This omission limits the capacity to account for local specificities, such as microclimatic variability, that play a determining role in the dynamics of defoliation. On the other hand, the cumulative effects of defoliation, which progressively weaken trees (Debaly et al., 2022; Paixao et al., 2019; Chen et al., 2017a) and can amplify the magnitude of subsequent outbreaks, remain relatively underexplored, making it difficult to identify management strategies that are well-adapted to real conditions. Moreover, the cumulative and lagged nature of defoliation damage, wherein each outbreak cycle builds on the weakened state induced by preceding cycles, demands advanced modeling techniques that simultaneously account for autocorrelation and spatial heterogeneity (Chen et al., 2017a; Debaly et al., 2022). Furthermore, the impact of extreme climate events — such as heatwaves and prolonged droughts — on SBW biology and the resulting defoliation of host species requires further research. These phenomena may initiate or reinforce medium to long-term feedback loops, affecting both outbreaks dynamics and the resilience of forest stands (Moise et al., 2019; Flower et al., 2014; Balducci et al., 2020). In light of these findings, an integrated approach is paramount. Employing models that capture the multiple levels of landscape heterogeneity, coupled with targeted studies conducted under varied conditions, will help develop more robust and effective management and adaptation strategies for SBW outbreaks.

The primary objective of this study is to investigate the dynamics of SBW-induced defoliation by exploring the interplay between climatic factors and landscape heterogeneity through the application of an adjacent-category autoregressive (ACAR) model for ordinal time series (Osse et al., 2023). This approach is particularly well-suited to capture the inherent characteristics of most defoliation data, notably its ordinal structure. We hypothesize that even when two spatially distinct sites exhibit the same level of defoliation, the underlying processes may diverge, thus warranting a departure from the conventional global modeling strategy. Instead of imposing a single, uniform model across the entire study region with shared parameters (Subedi et al., 2023; Navarro et al., 2018; Zhu et al., 2018; Eickenscheidt et al., 2019; Berguet et al., 2021), we analyze multiple landscape units, each subjected to distinct environmental conditions. This localized modeling approach improves our understanding of how site-specific ecological and climatic drivers influence defoliation dynamics. By comparing outcomes across these varied units, we gain insights into localized patterns of forest health and resilience, as well as the context-dependent effects of environmental stressors. We further employ clustering techniques to group landscape units based on similarities in the locally fitted models, thereby facilitating more targeted forest management strategies that address the unique needs and conditions of each cluster. Consequently, the proposed framework offers a region-specific decision-making tool for forest resource management, enhancing the effectiveness of interventions aimed at mitigating SBW-induced defoliation. Through these clusters, forest managers can prioritize interventions in landscape units where climatic pressure and defoliation trajectories are most severe, optimizing resource allocation and potentially mitigating future SBW damage.

2. Materials and methods

2.1. Study area

The study area is located within the boreal forests of Quebec, encompassing approximately 840,000 km^2. This region is characterized by vast coniferous forests, predominantly composed of balsam fir (*Abies balsamea*) and white spruce (*Picea glauca*), extending across latitudes 45° to 51°N and longitudes 65° to 80°W (Fig. 1). The regional climate is subpolar-subhumid continental, characterized by long, cold winters and short, cool summers. The north is colder and drier (mean annual temperature −7.5 °C, mean annual precipitation 500 mm/year), while the south is warmer and wetter (1 °C, 1000 mm/year). Subedi et al. (2023). This region exhibits high vulnerability to periodic SBW outbreaks (Cooke, 2024; Black et al., 2024; Boulanger and Arseneault, 2004). The ecological classification of Saucier et al. (2010) segments the study area into landscape units, defined as territories characterized by ecological homogeneity, shaped by factors such as topography, climate, and soil. Our investigation encompassed the totality of landscape units affected by the defoliation attributable to the SBW during the study period 1992–2022 (see Fig. 1). By focusing on all affected landscape units, we aimed to capture the variability of the severity dynamics and patterns of defoliation in different landscape units, thus providing a comprehensive understanding of the climatic impacts on the local dynamics of defoliation.

2.2. Data description

2.2.1. Defoliation data

The defoliation data used for this study consist of georeferenced polygons, which were delineated during aerial surveys of the defoliation damage caused by the SBW. These surveys are conducted annually across the province of Quebec. Each polygon is associated with defoliation class defined on the following ordinal scale: no defoliation (none), defoliation of the upper few tiers (light), defoliation of the upper half (moderate), and almost complete defoliation (severe). The collected defoliation data span each year from 1992 to 2022, inclusively, and are freely accessible through the Quebec Ministry of Natural Resources and Forests (MRNF, 2022).

For the purposes of this study, models were developed at the landscape unit scale. To obtain a single value of defoliation for each landscape unit on a given year, a spatial intersection was performed

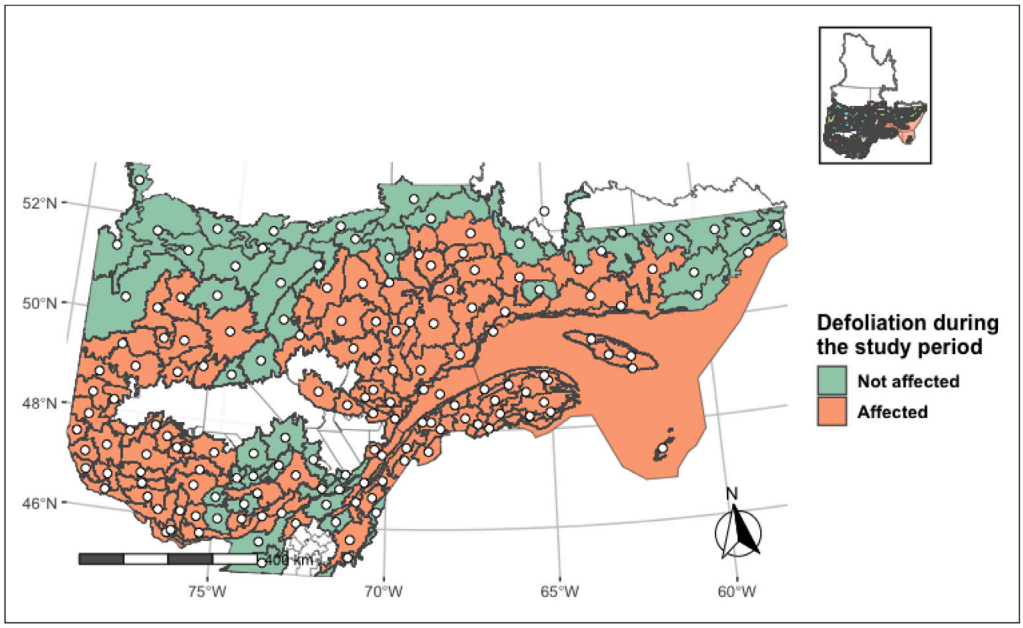

Fig. 1. Landscape units of the Quebec boreal forest included in this study.

between the defoliation polygons and the georeferenced polygons representing the landscape units, using the sf package (Pebesma, 2018). When multiple defoliation levels were present in a landscape unit on a given year, the defoliation level with the largest area within the landscape unit was chosen. Some landscape units experienced minimal defoliation, while in others, certain defoliation levels were absent during the study period. For the modeling process, we excluded landscape units that experienced no defoliation during the study period; for the remaining units, moderate and severe defoliation levels were amalgamated into a single category to increase the number of observations for each defoliation level. Consequently, three defoliation levels (none, light defoliation, and moderate/severe defoliation) were analyzed instead of the initially mentioned four.

2.2.2. Climate data sets

We used climate data derived from BioSIM (Fortin et al., 2022), a software tool designed to generate interpolated climate information from meteorological records adjusted to specific geographic locations and elevation. BioSIM integrates long-term climate normals with short-term weather data from meteorological stations, along with digital elevation data, to interpolate climate variables. BioSIM (version 11) was configured to retrieve climate data from nearby weather stations managed by meteorological agencies (e.g., Environment and Climate Change Canada). For each landscape unit (using the centroid of the landscape unit), it selected the nearest weather stations. Elevation data were incorporated from high-resolution digital elevation models to adjust for topographic variation in temperature and precipitation, improving the accuracy of localized climate estimates.

We extracted elevation and a suite of key climate variables for each study location, including daily maximum and minimum temperatures, daily precipitation, daily relative humidity, daily solar radiation, daily wind speeds at 2 m and 10 m above ground, and daily snow data. To reflect the biological characteristics of the spruce budworm (SBW) and align with prior studies (Debaly et al., 2022; Volney and Fleming, 2007, 2000; Osse et al., 2023), daily maximum and minimum temperatures were seasonally aggregated for spring and summer. Given the high correlation between daily relative humidity and daily precipitation, as well as between daily wind speeds at 2 m and 10 m, we aggregated these variables to simplify subsequent analyses. Specifically, daily precipitation was aggregated as total annual precipitation, and daily wind speed at 10 m was represented as annual wind speed variation at the same height. Spring was defined as April, May, and June, while summer comprised July, August, and September.

For the purposes of this study, we focused on the following climate variables: the range (maximum - minimum) of daily maximum temperature during the summer (*Tmax. summer*), the range of daily maximum temperature during spring (*Tmax. spring*), the range of daily minimum temperature during summer (*Tmin. summer*), the range of daily minimum temperature during spring (*Tmin. spring*), the logarithm of total annual precipitation (*logTotprec*), the annual range of wind speed at 10 m (*Wind speed at 10* m), the average annual solar radiation (*Solar radiation*), and the total annual snowfall (*Snow*). Quadratic terms were included for temperature-related variables (*Tmax. summer*, *Tmax. spring*, *Tmin. summer*, and *Tmin. spring*) to account for potential non-linear climate effects. We prioritized predictors that (i) map directly onto SBW physiology and host–insect phenology, (ii) summarize *seasonal* exposure windows that matter biologically, and (iii) keep models parsimonious. Seasonal ranges of daily minima and maxima (spring/summer) capture tolerance windows, phenological pacing, and heat- or cold-stress amplitudes affecting larval development, host budburst, and synchrony. Annual precipitation (log-scaled) summarizes moisture availability and correlates with humidity regimes that can mediate larval performance and pathogen pressure. Wind at 10 m integrates dispersal and dislodgement mechanisms for first-instar larvae. Solar radiation and snowfall approximate, respectively, energy input (affecting microclimate and host tissue quality) and overwintering context. Quadratic temperature terms were included a priori to detect threshold-like responses consistent with physiological and synchrony constraints, while avoiding proliferation of highly collinear derived metrics.

2.3. Modeling

For each landscape unit, we fitted an adjacent-category autoregressive model (Osse et al., 2023) with all possible combinations of our covariates. The model is defined as:

$$Y_{k,t} = \mathbb{1}\left\{\sum_{k=0}^{j-1}\pi_{k,t} \le U_t < \sum_{k=0}^{j}\pi_{k,t}\right\}, \quad 0 \le j \le K, \tag{1}$$

$$\log\frac{\pi_{j,t}}{\pi_{j-1,t}} =: \eta_{j,t} = \omega_j + \gamma^\top X_{t-1} + \alpha^\top \overline{Y}_{t-1} + \beta_j \eta_{j,t-1}, \quad 1 \le j \le K, t \in \mathbb{Z}, \tag{2}$$

where:

$\omega_j \in \mathbb{R}, \gamma \in \mathbb{R}^P, \alpha \in \mathbb{R}^K$ and $\beta_j \in \mathbb{R}^*$ for $j = 1, \ldots, K$.

ω_j: is the intercept for category j,

γ: represents the effect of covariates (e.g., temperature, precipitation),

α: captures the autoregressive influence of severity from the prior year and

β_j: extends the autoregression beyond a lag of 1.

Model adequacy was assessed using a Portmanteau test with lag 1, as described in Osse et al. (2023). The test tests whether the first-order residual autocorrelations are jointly zero—*i.e.*, whether the fitted model has left any serial dependence unexplained. Only models for which the Portmanteau test did not reject the adequacy were considered. We selected the best model for each landscape unit using the information criterion *AIC*.

2.4. Clustering

For any landscape unit i, we denote as $(X_t^{(i)}, Y_t^{(i)})$ the dataset that yielded the best model U_i with the estimated values of the parameters $\theta^{(i)} = (\omega^\top, \mathrm{vec}(\Gamma)^\top, \alpha^\top, \beta_1, \ldots, \beta_K)^\top$, k_i the number of estimated parameters in the model U_i and AIC_i its Akaike information criterion. Given two landscape units a and b, we have:

- for the dataset $X_t^{(a)}$ of landscape unit a, the best model is U_a with its Akaike Information Criterion AIC_a;
- for the dataset $X_t^{(b)}$ of landscape unit b, we have a different model U_b with its Akaike Information Criterion AIC_b;
- using model U_a as-is (same values of the parameters $\theta^{(a)}$, without re-fitting the model), we calculate its likelihood ($\mathcal{L}$) with the data $X_t^{(b)}$ to obtain the corresponding Akaike Information Criterion, denoted AIC_{ba} denoted $AIC_{ba} = 2k_a - 2\ln(\mathcal{L}(\theta^{(a)}|X_t^{(b)}))$;
- similarly, we take model U_b and calculate its likelihood with the data $X_t^{(a)}$, resulting in the corresponding Akaike Information Criterion AIC_{ab} denoted $AIC_{ab} = 2k_b - 2\ln(\mathcal{L}(U_b|X_t^{(a)}))$.

We also denote as $d_{a,b}$ the distance between U_a and U_b the respective best models of landscape units a and b. Our distance is given by:

$$d_{a,b} = \sqrt{(AIC_{ba} - AIC_b)^2 + (AIC_{ab} - AIC_a)^2}$$

In other words, we define a distance between models such that the distance is small if the best model for landscape unit a provides a good fit to the data of landscape unit b and vice versa. Clusters of landscape units were then identified from the pairwise distance matrix $d_{a,b}$ using hierarchical clustering with Ward's minimum-variance method (Murtagh and Legendre, 2014).

2.5. Statistical characteristics of clusters and assessment of clustering quality

2.5.1. Statistical characteristics of clusters

The optimal number of clusters was determined by inspecting the Ward-linkage dendrogram. To discern the distinguishing features of each group, a comprehensive statistical analysis of the environmental and climatic variables was executed. Key variables such as elevation, seasonal temperature ranges (both maximum and minimum), humidity, wind speed, solar radiation, precipitation, and snow cover were chosen due to their ecological significance and potential impact on SBW defoliation dynamics. For each group, the means and standard deviations of these variables were computed to encapsulate the central tendencies and variability. A boxplot was constructed to visualize the mean values of these variables across clusters, facilitating direct comparisons. To evaluate the statistical significance of differences between the groups, we employed Analysis of Variance (ANOVA) (Stahle et al., 1989) for each variable, using the cluster assignments as the grouping factor. Variables exhibiting a p-value below the significance threshold of 0.05 were considered significantly different between groups. For these variables, a post hoc Tukey's Honest Significant Difference (HSD) test (Abdi and Williams, 2010) was conducted to identify which clusters differed in a pairwise manner.

2.5.2. Assessment of clustering quality

The clustering quality was evaluated employing the silhouette method (Dudek, 2020), which assesses cluster cohesion and separation. Initially, a Euclidean distance matrix was computed for the scaled numerical variables to quantify the dissimilarities among the landscape units. Subsequently, for each observation, the silhouette coefficient was computed using the formula:

$$S(i) = \frac{b(i) - a(i)}{\max(a(i), b(i))}$$

where $a(i)$ signifies the average distance between observation i and all other points within the same cluster, and $b(i)$ indicates the minimum average distance between observation i and all other groups. The silhouette coefficient ranges from −1 to 1, where values approaching 1 denote strong clustering, values near 0 indicate boundary observations, and negative values suggest potential misclassification. The average silhouette width was determined as a global measure of cluster quality, with higher values indicating better-defined clusters. To visualize the results, a silhouette plot was generated, with each cluster represented by a distinct color, and the average silhouette width marked by a vertical dashed line. This visualization offered insights into the cohesion within clusters and the separation between clusters, thereby facilitating the identification of poorly defined or overlapping clusters.

2.6. Implementation and tools

All statistical analyses and inference methods were implemented in *R language version 4.4.2* (R Core Team, 2024). The following packages were used for data manipulation, analysis, and visualization: `dplyr` (Wickham et al., 2023), `tidyr`, `tibble`, and `ggplot2` for data handling and creating boxplots; `cluster` (Maechler et al., 2013) for silhouette analysis; `factoextra` (Kassambara and Mundt, 2017) and `dendextend` for cluster visualization and customization; `sf` (Pebesma, 2018) and `ggspatial` for geospatial data handling and mapping; `raster` for raster data manipulation; `multcompView` to display multiple comparisons with letter-based grouping; `ggthemes` and `viridis` for additional themes and color palettes; `grid` and `cowplot` for advanced plot layout manipulation; and `conflicted` to manage naming conflicts between packages. The significance of the results was evaluated at the 5% threshold ($\alpha = 0.05$). All scripts and data sets are available in the repositories mentioned in the Data Availability Statement, ensuring reproducibility.

3. Results

This section presents how landscape-level models of SBW defoliation were fitted and then clustered based on their similarity, highlighting both the influential climatic covariates identified and the resulting spatial patterns of defoliation. In this study, the ACAR model was implemented on individual landscape units, which were subsequently aggregated into clusters based on similarities of the fitted models. Models in the same cluster thus show similar defoliation dynamics, including the effects of environmental variables on defoliation.

3.1. Climatic influences and defoliation dynamics

The coefficients of the best model for each landscape unit are presented in Table 1. The variation in minimum temperature during summer is the most influential climatic variable across the majority of landscape units (Fig. 2). In numerous units, these models integrate parameters associated with the seasonal range of daily maximum and

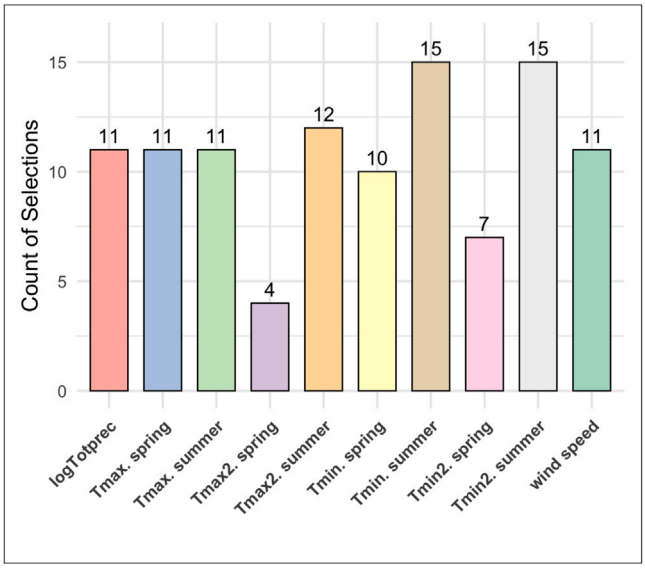

Fig. 2. Frequency of variable selection.

minimum temperatures, thus highlighting not only the non-linear relationship between temperature and defoliation but also the seasonal specificity of these effects. This underscores the diverse interactions between climatic factors and ecological processes dependent on the season. For example, in regions such as Lac la Blanche and Mont-Laurier, the coefficients for spring and summer temperatures exhibit a quadratic effect. For summer temperatures, a maximum threshold becomes apparent, indicating that elevated temperatures beyond a particular range correlate with reduced defoliation. For certain units (for example, Lac Mékinac and Réservoir Pipmuacan), significant feedback parameters, particularly β, indicate strong autoregressive dependencies. This implies that the dynamics of defoliation in these landscape units are influenced by antecedent conditions, suggesting the cumulative impact of defoliation over time on forest health. In Port-Menier, the models demonstrate a pronounced effect of spring temperatures, where a wider range of spring temperatures leads to increased defoliation. Moreover, in Monts Groulx and Petit Lac Manicouagan, summer temperature thresholds exhibit a nuanced relationship: increased variability in summer temperatures is linked to reduced defoliation up to a certain threshold, beyond which the trend reverses, resulting in increased defoliation.

We also found that wind speed and precipitation exert contrasting, generally milder impacts on defoliation compared to temperature, yet they vary substantially across different landscape units. For instance, when wind speed at 10 m emerges as a significant factor, it can either increase (e.g., Mont-Laurier) or decrease (e.g., Lac du Poisson Blanc) the probability of defoliation depending on local conditions. Precipitation likewise exhibits notable variability: positive effects are observed in certain units (e.g., Saint-Jérôme) and negative effects in others (e.g., Réservoir Pipmuacan). Overall, these results underscore the need to consider wind speed and precipitation locally in defoliation models, given that their impacts are strongly tied to each landscape's distinct ecological context.

3.2. Cluster heterogeneity

The clustering of landscape units based on their models of defoliation dynamics (Fig. 3) and the characterization of these clusters (Fig. 4) have revealed a broad spectrum of SBW-induced defoliation patterns in boreal forests, intricately shaped by different environmental factors. Among the five identified clusters, clusters 4 and 5 stand out for their homogeneous climatic and topographic conditions, with positive silhouette scores (0.55 and 0.24, see Fig. 5). Cluster 4, located in low-altitude zones with minimal thermal variation and high precipitation, indicates stable climatic conditions that reduce the vulnerability of SBW. Conversely, cluster 5, characterized by high altitudes, significant thermal variation, high solar exposure, and low snow cover, reflects extreme conditions where SBW activity is less predictable, requiring tailored adaptive management strategies. Fig. 6 depicts the spatial distribution of landscape units, highlighting their arrangement across the study area.

In contrast, clusters 1, 2, and 3 exhibit negative silhouette scores (−0.43, −0.32, and −0.24, Fig. 5), suggesting overlaps and heterogeneous characteristics. These clusters represent intermediate conditions, ranging from areas with significant wind exposure and moderate humidity (cluster 1), to low-altitude zones with low precipitation and humidity (cluster 2), to highly diverse landscapes that need further segmentation (cluster 3). These findings highlight the critical role of climatic factors such as altitude, thermal amplitude, humidity, and wind in shaping SBW defoliation patterns and provide actionable insights for developing differentiated forest management strategies.

4. Discussion

4.1. The multifaceted impacts of climate on the defoliation dynamics

While numerous studies have shown that rising temperatures attributable to climate change are correlated with increases in both the frequency and intensity of SBW outbreaks (Overpeck et al., 1990; Régnière and Nealis, 2007; Pureswaran et al., 2015; Bouchard and Auger, 2014; Bouchard et al., 2018; Moise et al., 2019; Pureswaran et al., 2019), our model results demonstrate a complex and non-linear association between temperature and SBW defoliation dynamics. This complex relationship may arise from the combined influence of physiological (Bellemin-Noël et al., 2021; Deslauriers et al., 2019; Howe et al., 2024), phenological (Eveleigh and Johns, 2014; Deslauriers et al., 2019), and ecological factors (Zhang et al., 2018) that drive SBW behavior, highlighting the importance of understanding how climate change modifies defoliation patterns during SBW outbreaks. Existing ecological literature associated warmer summers with increased larval mortality or delays in defoliation cycles (Abarca and Lill, 2015; Ward et al., 2019; Portalier et al., 2024; Delisle et al., 2022). Our results emphasize the complex role that temperature plays in shaping the defoliation dynamics. In specific landscape units, the models offer supplementary insights. Although initially beneficial to SBW populations (Régnière and Nealis, 2019; Bellemin-Noël et al., 2021), rising temperatures can precipitate a series of physiological stresses and ecological mismatches that ultimately constrain their success (Howe et al., 2024; Portalier et al., 2024). These findings suggest that temperature-related variables (e.g., *Tmin. summer*) play a dual role: they can promote SBW development up to a threshold but can also hinder larval survival beyond it. This threshold-like behavior further reflects the non-linear impact of extreme temperatures on physiological processes (e.g., dehydration, metabolic stress) in SBW larvae.

A pivotal mechanism affecting SBW dynamics under increasing temperatures is the disruption of phenological synchrony between the budworm's life stages and the bud burst of its host trees. Premature bud bursts in species such as black spruce (*Picea mariana*) and balsam fir (*Abies balsamea*) may not coincide with larval emergence, leading to mismatches that diminish larval survival (Pureswaran et al., 2019; Portalier et al., 2024; Howe et al., 2024). Black spruce, due to its inherently delayed bud burst, becomes less susceptible to defoliation in warmer climates, as larvae may emerge before adequate foliage becomes available for consumption (Pureswaran et al., 2015). This phenomenon highlights the existence of a defoliation threshold, wherein excessive warming reduces defoliation rates due to disrupted synchrony. This interpretation provides a compelling explanation for

Table 1
Estimation of the best selected models for each landscape unit.

Landscape units	Parameters																	
	ω_1 (sd)	ω_2 (sd)	Tmax. spring (sd)	Tmax. summer (sd)	Tmin. spring (sd)	Tmin. summer (sd)	wind speed at 10m (sd)	$logTapprec$ (sd)	$Tmin.^2$ spring (sd)	$Tmax.^2$ spring (sd)	$Tmin.^2$ summer (sd)	$Tmax.^2$ summer (sd)	α_1 (sd)	α_2 (sd)	β_1 (sd)	β_2 (sd)	portemanteau stat	portemanteau p-value
Lac la Blanche	−10.68 (3.48)	−11.48 (3.34)	0.82 (0.30)	−1.70 (0.62)	–	–	–	–	–	–	0.30 (0.11)	–	2.25 (1.19)	4.45 (2.46)	0.76 (0.20)	−0.14 (2.14)	1.03	0.60
Mont-Laurier	−60.89 (29.14)	−64.43 (29.56)	−3.55 (0.53)	–	–	–	179.94 (47.21)	–	–	–	−0.37 (0.10)	−0.62 (0.11)	7.56 (5.61)	−6.77 (1.76)	0.94 (0.05)	0.25 (0.14)	0.32	0.85
Lac du Poisson Blanc	−181.51 (11.92)	−284.52 (12.97)	5.47 (0.54)	–	–	126.85 (10.23)	−326.21 (49.38)	–	−0.57 (0.05)	–	−11.52 (0.93)	–	208.96 (18.21)	327.46 (29.44)	−0.97 (0.01)	−0.49 (0.04)	0.05	0.97
Saint-Jérôme	−61.48 (12.05)	−179.28 (10.32)	–	−53.84 (3.84)	–	–	–	206.14 (9.96)	−0.17 (0.02)	–	–	3.36 (0.28)	30.85 (2.28)	138.36 (9.72)	0.39 (0.03)	−0.99 (0.01)	0.03	0.98
Lac Mékinac	−530.11 (141.06)	−532.07 (141.41)	–	−10.50 (3.67)	–	11.24 (2.62)	434.70 (105.22)	37.31 (26.57)	−0.08 (0.08)	–	–	–	103.98 (44.25)	98.05 (37.54)	0.76 (0.02)	−0.83 (0.29)	0.42	0.81
Tadoussac	−41.20 (56.82)	−49.25 (66.14)	7.15 (0.70)	–	–	−190.06 (61.62)	298.97 (165.18)	47.66 (14.39)	–	–	17.03 (5.21)	–	−14.56 (6.80)	13.98 (33.59)	0.81 (0.14)	0.80 (0.18)	0.00	1.00
Plaine du lac Saint-Jean	−37.40 (4.12)	−194.45 (4.76)	–	−34.60 (2.43)	−7.65 (0.19)	–	143.72 (2.98)	–	–	–	−1.57 (0.06)	3.70 (0.17)	151.79 (3.43)	317.82 (5.66)	−0.60 (0.04)	−0.93 (0.01)	0.01	0.99
Réservoir Pipmuacan	9.08 (4.45)	−0.33 (2.74)	–	–	–	–	–	−10.09 (4.51)	–	0.01 (0.02)	–	–	16.60 (7.91)	25.80 (9.44)	0.87 (0.32)	0.54 (0.21)	0.04	0.98
Lac des Savanes	−2.78 (28.25)	−9.22 (32.51)	–	−27.50 (6.17)	–	–	56.10 (27.59)	–	–	–	–	2.22 (0.49)	−2.97 (3.92)	−2.74 (4.63)	0.82 (0.13)	0.70 (0.27)	0.31	0.85
Forestville	−166.40 (44.53)	−168.37 (46.28)	5.98 (1.40)	–	–	–	58.77 (15.36)	–	–	–	–	–	25.52 (9.16)	−1.43 (5.77)	0.85 (0.07)	0.95 (0.05)	0.00	1.00
Lac au Loup Marin	−419.16 (51.48)	−426.88 (48.77)	–	–	−12.95 (1.21)	227.09 (13.45)	–	–	–	–	−20.26 (1.02)	–	1.88 (10.12)	0.44 (12.30)	0.91 (0.03)	0.88 (0.06)	0.00	1.00
Lac Dionne	−321.89 (47.14)	−404.73 (52.07)	2.54 (0.72)	–	–	−1.23 (0.46)	–	199.37 (35.38)	–	–	–	–	132.10 (12.59)	212.41 (18.62)	−0.61 (0.11)	−0.89 (0.02)	0.00	1.00
Sept-Îles	−387.45 (22.31)	−494.45 (31.78)	–	−6.00 (0.67)	13.66 (1.04)	−6.56 (0.61)	–	–	–	–	–	–	419.57 (26.84)	459.55 (29.17)	−0.91 (0.01)	−0.80 (0.02)	0.03	0.99
Port-Menier	36.61 (12.60)	23.29 (13.51)	–	30.79 (4.49)	0.69 (0.94)	–	–	−150.09 (8.00)	–	–	–	–	−128.43 (11.14)	−31.06 (2.27)	0.98 (0.01)	0.67 (0.02)	0.16	0.92
Rivière Jupiter	−1190.21 (80.05)	−1193.18 (80.11)	–	297.07 (22.05)	−14.05 (1.44)	8.88 (0.66)	399.43 (23.43)	–	–	–	–	−28.46 (1.98)	27.86 (1.83)	8.48 (3.54)	0.79 (0.02)	0.81 (0.01)	0.23	0.89
Rivière aux Saumons	−725.05 (87.94)	−741.87 (89.87)	5.36 (0.53)	278.55 (39.54)	−4.28 (0.61)	−42.05 (7.84)	43.13 (8.18)	−26.65 (13.45)	–	–	3.95 (0.74)	−24.35 (3.42)	13.31 (1.93)	9.56 (2.41)	0.42 (0.03)	−0.31 (0.07)	0.20	0.90
Lac Manouane	−328.60 (9.22)	−372.34 (10.32)	32.28 (1.40)	−123.49 (11.34)	–	−33.43 (2.54)	–	–	–	–	13.43 (0.50)	2.06 (0.39)	448.88 (24.91)	259.49 (23.18)	−0.47 (0.01)	−0.64 (0.01)	0.00	1.00
Lac Rouvray	−409.58 (57.16)	−477.51 (67.36)	–	–	–	137.83 (18.99)	–	–	–	–	−11.13 (1.54)	–	65.44 (10.82)	112.44 (21.33)	0.49 (0.07)	0.31 (0.08)	0.01	0.99
Lac du Sault aux Cochons	−119.16 (10.68)	−234.62 (13.43)	−8.87 (0.48)	–	–	–	–	112.53 (9.62)	–	–	–	–	207.59 (10.03)	331.01 (16.76)	−0.96 (0.01)	−0.98 0.01	0.00	1.00
Lac Dissimieux	43.47 (9.69)	−23.77 (2.33)	–	–	–	–	–	–	−0.24 (0.04)	–	0.32 (0.02)	−0.43 (0.09)	11.28 (1.84)	111.81 (15.78)	0.71 (0.05)	−0.95 (0.03)	0.15	0.93
Lac Guinecourt	−167.07 (79.27)	−257.71 (103.97)	–	–	–	92.24 (36.58)	–	−40.63 (11.67)	–	–	−9.77 (3.64)	–	98.36 (36.90)	119.15 (220.98)	0.86 (0.02)	−0.99 (0.02)	0.13	0.94
Lac Carteret	141.00 (22.66)	−87.15 (46.12)	−24.85 (2.33)	–	–	–	−116.35 (17.47)	–	0.99 (0.08)	–	–	–	483.52 (16.02)	352.34 (17.67)	−0.85 (0.03)	0.66 (0.02)	0.00	1.00
Réservoir Manic 3	−478.35 (15.81)	−542.20 (15.28)	–	–	–	164.05 (5.83)	174.32 (6.21)	−285.53 (12.36)	–	–	−12.68 (0.49)	−1.59 (0.06)	156.11 (8.62)	308.27 (11.81)	−0.83 (0.01)	−0.63 (0.01)	0.00	1.00
Lac Berté	47.36 (16.02)	−46.78 (6.93)	–	–	–	–	–	–	−0.50 (0.16)	–	–	–	249.51 (64.14)	111.57 (35.65)	−0.06 (0.33)	0.69 (0.01)	0.14	0.93
Lac Sainte-Anne	62.19 (6.92)	29.24 (23.04)	–	–	–	–	–	−80.16 (6.32)	–	–	0.50 (0.07)	−0.71 (0.14)	221.90 (42.66)	78.50 (18.19)	−0.79 (0.03)	0.83 (0.02)	0.00	1.00
Lac Walker	−22.11 (5.17)	−73.64 (4.59)	–	–	0.79 (0.28)	−12.06 (0.73)	–	–	–	–	–	–	317.19 (13.91)	127.36 (6.82)	−0.80 –	0.77 (0.01)	0.00	1.00

(*continued on next page*)

Table 1 (*continued*).

Réservoir Manicouagan	−7.04 (3.26)	−14.66 (6.93)	–	–	–	–	–	–	–	−0.22 (0.09)	–	0.89 (0.23)	55.46 (21.95)	−1.36 (10.09)	0.59 (0.20)	0.73 (0.12)	0.09	0.95
Monts Groulx	−767.70 (52.66)	−924.03 (66.89)	70.55 (5.13)	–	−32.81 (2.48)	–	–	–	–	–	–	–	366.70 (28.28)	422.45 (33.86)	−0.39 (0.03)	−0.79 (0.01)	0.01	1.00
Lac Grandmesnil	−40.43 (5.71)	−459.21 (46.59)	–	–	–	–	–	–	–	−0.45 (0.02)	–	−0.78 (0.05)	412.74 (46.96)	670.93 (87.56)	−0.95 (0.01)	−0.95 (0.01)	0.00	1.00
Lac Nipissis	132.71 (150.66)	108.48 (134.40)	–	6.65 (5.38)	−29.89 (14.40)	32.10 (7.80)	–	–	–	–	–	–	10.06 (7.86)	16.17 (31.54)	0.96 (0.07)	0.74 (0.27)	0.00	1.00
Havre-Saint Pierre	−15.10 (1.09)	−155.15 (11.64)	–	–	–	–	–	–	−0.16 (0.01)	–	−0.65 (0.05)	–	384.12 (31.84)	176.94 (11.38)	−0.86 (0.02)	0.84 (0.03)	0.21	0.90
Lac Pécaudy	10.49 (2.79)	−64.54 (7.96)	–	–	8.10 (1.10)	−11.96 (1.37)	–	–	–	−0.53 (0.06)	–	–	108.74 (10.55)	122.39 (11.26)	−0.50 (0.04)	−0.98 0.01	0.00	1.00
Petit lac Manicouagan	35.41 (2.69)	33.35 (5.46)	–	–	–	–	–	–	–	−0.53 (0.02)	−1.18 (0.05)	–	171.20 (7.68)	−19.80 (1.83)	−0.90 (0.02)	0.62 (0.02)	0.24	0.89

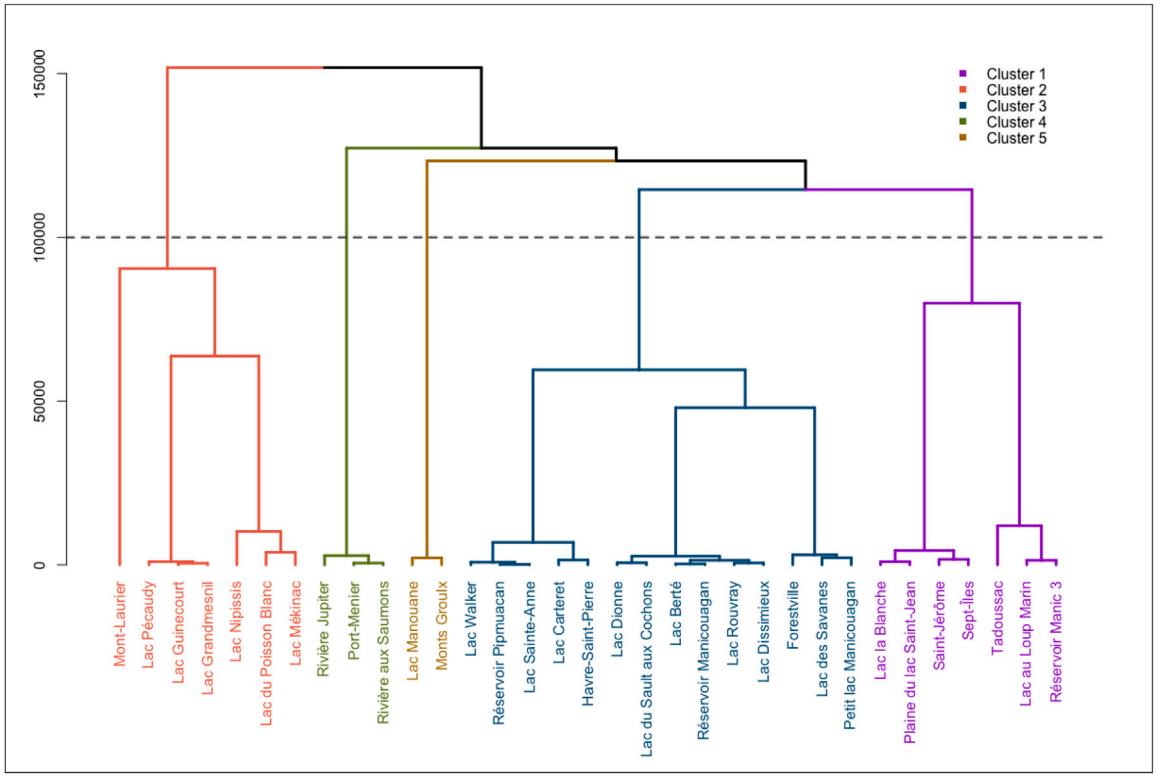

Fig. 3. Dendrogram of landscape units hierarchical clustering.

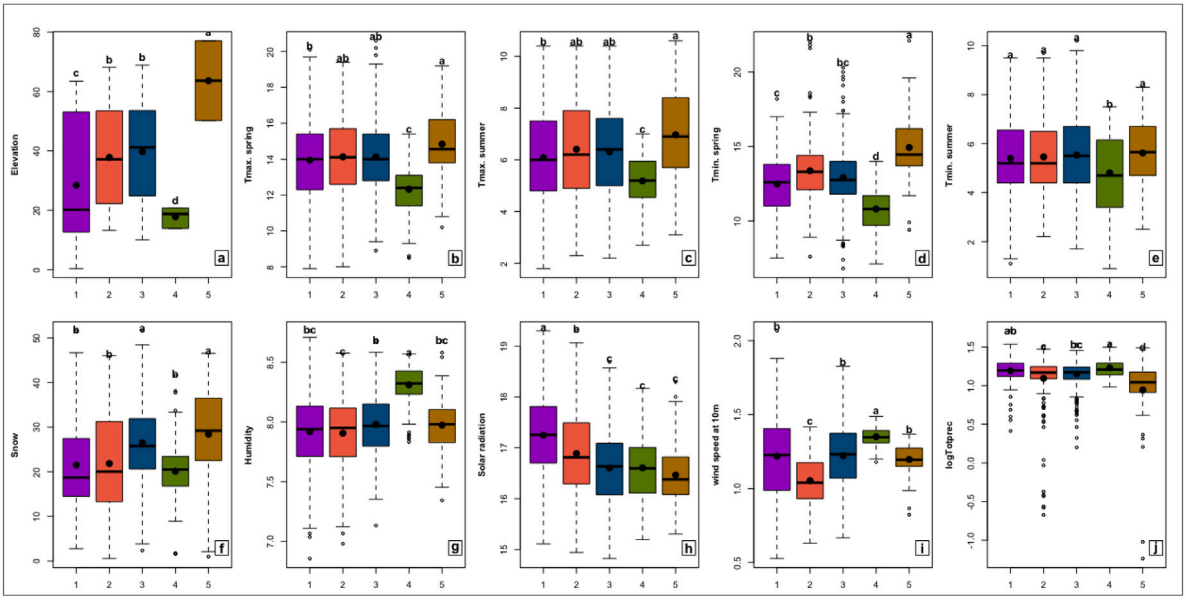

Fig. 4. The distribution of significant environmental variables across clusters. Each boxplot represents a specific variable's variation among the five clusters. The black points within each box denote the mean values of the variable for the corresponding cluster. Compact letter displays (above the boxes) indicate significant differences between clusters based on post-hoc Tukey tests.

the quadratic effects observed in our model, emphasizing the complex and non-linear relationships among key variables.

In parallel to the effect of temperature on SBW-host synchrony, temperature-induced physiological stress emerges as a critical factor limiting SBW populations (Régnière and Nealis, 2019; Bouchard et al., 2018). As temperatures rise, metabolic rates in ectothermic organisms such as the SBW accelerate, thereby increasing energy demands that may not be sustainable under suboptimal conditions (Goodhue et al., 2017; Reichenbach and Stairs, 1985; Hayes et al., 2015). This is particularly evident during critical life stages, such as larval feeding, where high temperatures lead to reduced nutrient absorption, dehydration, and impaired growth (Bellemin-Noël et al., 2021; Nealis and Régnière, 2004). Additionally, extreme temperatures disrupt reproductive success by diminishing egg viability and altering timing, further constraining population growth (Candau et al., 2018; Ren et al., 2020). Furthermore, the responses of host trees to rising temperatures significantly influence

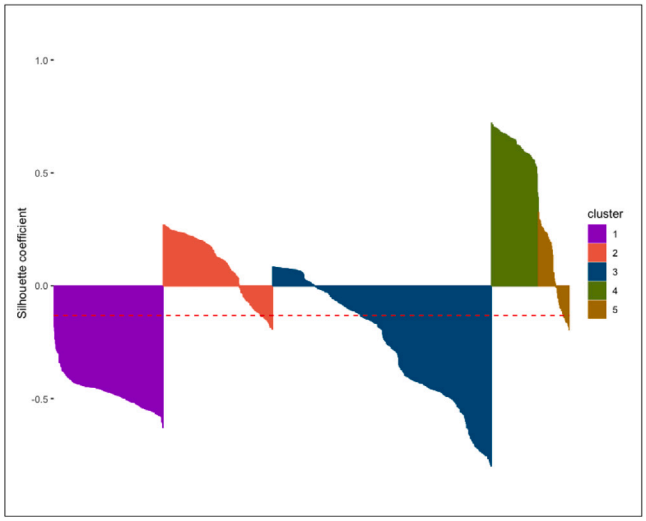

Fig. 5. Silhouette analysis of cluster performance.

SBW survival and development. Elevated temperatures expedite foliage maturation, resulting in tougher and less nutritious leaves, thereby reducing their suitability for larvae (Eveleigh and Johns, 2014). Compounding this effect, temperature-induced changes in foliage chemistry, such as increased levels of secondary metabolites like phenolics and terpenes, degrade food quality even further, intensifying physiological stress in larvae (Despland et al., 2011). Consequently, these nutritional limitations hinder larval growth and survival, ultimately reducing population viability.

Localized microclimatic conditions further exacerbate SBW outbreak dynamics. For instance, drier or warmer microclimates intensify water stress in host trees, accelerating the decline in foliage quality and availability (Zhang et al., 2018). This spatial variability in habitat suitability not only alters the geographical extent and intensity of outbreaks but also contributes to regional variations in the processes driving defoliation dynamics, as reflected in different landscape-based models. Taken together, these findings emphasize the urgent need for adaptive forest management strategies to mitigate the impacts of SBW outbreaks in the context of a changing climate. On one hand, monitoring phenological shifts in host trees is essential to enhance forest resilience; on the other hand, identifying temperature thresholds that constrain SBW populations is equally critical for refining predictive models. In some landscape units, spring temperatures lead to increased defoliation. This pattern agrees with the hypothesis that warmer springs may precipitate the early emergence of larvae, thereby exacerbating damage from defoliation (Régnière et al., 2012; Bellemin-Noël et al., 2021; Delisle et al., 2022; Rose and Blais, 1954; Moise et al., 2024).

Our findings also underscore that, while temperature is widely recognized as a fundamental determinant of SBW dynamics (Pureswaran et al., 2015; Régnière and Nealis, 2019), additional climatic factors such as wind speed and precipitation can play a significant context-dependent role (Royama, 1984). Higher wind speeds often facilitate the dispersal of first instar larvae by allowing them to bridge between host trees (Beckwith and Burnell, 1982; Ramachandran, 1987; Anderson and Sturtevant, 2011), but strong gusts can also dislodge larvae, reducing their chances of survival (Jennings et al., 1983). This dual effect is clearly illustrated by the contrasting coefficients in Mont-Laurier (positive effect) and Lac du Poisson Blanc (negative effect). Precipitation similarly exerts a range of impacts: excessive rainfall can reduce larval feeding efficiency or encourage entomopathogenic fungal outbreaks (Subedi et al., 2023), whereas heightened humidity can in some contexts bolster larval survival (Bouchard et al., 2018). Given that these variables demonstrate markedly different influences across landscape units — positive in Saint-Jérôme vs. negative in Réservoir Pipmuacan — local ecological factors such as stand composition, topography, and microclimatic conditions likely mediate these processes. Consequently, incorporating wind speed and precipitation into defoliation models on a site-by-site basis is essential for accurately predicting SBW outbreaks and tailoring more effective forest management strategies.

4.2. Methodological contributions and novelty

While our results reaffirm the documented influences of temperature and precipitation on SBW dynamics, the principal contribution of this study is methodological. We extend and operationalize the adjacent-category autoregressive (ACAR) framework (Osse et al., 2023) for ordinal defoliation time series, bringing together three properties rarely combined in outbreak analyses. First, it respects the ordered, categorical scale of defoliation by modeling adjacent-category log-odds, thereby avoiding the information loss inherent to arbitrary dichotomization or continuous approximations (Agresti and Kateri, 2011; Bürkner and Vuorre, 2019). Second, it embeds temporal dependence through an explicit AR(1) structure on the linear predictor, directly capturing epidemic memory and state persistence—an element often highlighted as missing in conventional outbreak models (Royama, 1984; Sturtevant et al., 2015). Third, it remains fully interpretable, with coefficients mapping to odds ratios that govern transitions between neighboring defoliation states, in contrast to the opacity of many machine-learning approaches increasingly applied to forest-disturbance data (Hanberry, 2022). Taken together, these features distinguish the ACAR framework from conventional logistic, multinomial, or generalized additive approaches, which typically neglect at least one of these dimensions (Wood, 2017; Subedi et al., 2023; Régnière and Nealis, 2019).

Within this framework, the temperature response was modeled as a quadratic curve, which makes it possible to identify a thermal optimum — or tipping range — beyond which the risk of outbreak intensification becomes highest. The steepness of the curve around this optimum reflects the system's sensitivity, indicating how strongly defoliation dynamics respond to small shifts in temperature. These parameters provide immediate ecological meaning and management relevance: they delineate the ranges of temperature where interventions are most critical and where forest systems may undergo non-linear shifts toward elevated defoliation risk (Moise et al., 2019; Pureswaran et al., 2019). Explicitly detecting such thresholds directly answers recent calls for models capable of identifying non-linear ecological responses to climate change (Seidl et al., 2017; Thom, 2023).

Beyond the single-site modeling, we complement the ACAR with a clustering procedure based on a bidirectional AIC distance between fitted models. Unlike traditional groupings based on static abiotic descriptors, this method partitions landscapes according to the *functional similarity* of their outbreak dynamics. This information-theoretic approach follows the philosophy of Burnham and Anderson (2002), where AIC is used not only for single-model selection but also as a comparative measure of model fit across competing hypotheses. By extending this logic to a cross-application of fitted models, our framework explicitly evaluates how well the process governing one landscape can explain the data from another. This is conceptually aligned with the perspective of Hilborn and Mangel (1997), who emphasize confronting ecological models with empirical data as a critical step in evaluating their generality and transferability. The resulting clusters encode ecological memory, reveal policy-relevant thresholds (via T^* and curvature), and align directly with site-specific climatic pressures.

Taken together, this methodological contribution advances both theory and practice. It provides a general and extensible statistical tool for ordinal ecological time series — such as disease-severity scales, drought categories, fire-danger indices, avalanche-danger ratings, air-quality index classes, trophic-state classifications of lakes,

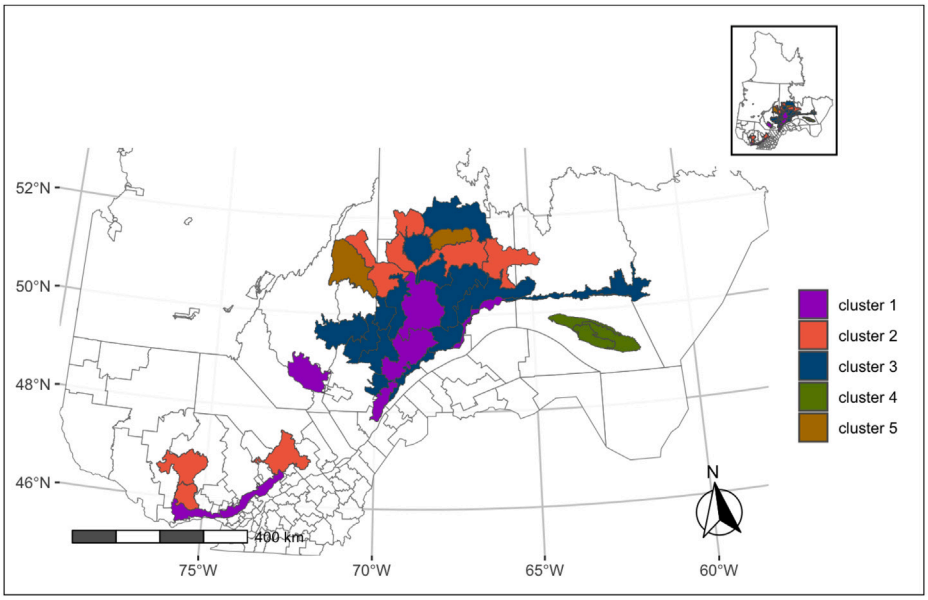

Fig. 6. Mapping clustered landscape units.

harmful-algal-bloom severity levels, coral-bleaching alert stages, river ecological-integrity classes, ordinal abundance categories, and aggregated phenological stages (Tramblay et al., 2020; Jolly et al., 2015) — while simultaneously offering an actionable framework for forest management, enabling differentiated interventions at the landscape-unit scale.

4.3. Legacy effects of historical defoliation events

Our findings indicate that defoliation dynamics within a given landscape unit depend not only on the current year's climatic conditions but also on the cumulative defoliation that occurred earlier in the same outbreak cycle. The significant autoregressive terms reflect this legacy effect: each successive year of moderate or severe defoliation further weakens host trees, thereby increasing their likelihood of sustaining additional damage as the epidemic wave progresses (Nealis and Régnière, 2021; Debaly et al., 2022; Osse et al., 2023). Persistent defoliation can lead to a reduction in the photosynthetic capacity of a tree, the depletion of its energy reserves, and the limitation of its recovery capabilities, increasing its vulnerability to additional stressors such as drought, secondary pests, or diseases (Wang et al., 2021; O'Connell and Wiley, 2024; Deslauriers et al., 2019). In addition, this cumulative effect can trigger a feedback loop in which declining forest health increases the likelihood of further defoliation, thus amplifying the long-term effects on forest structure and composition (Régnière and Nealis, 2007; Chen et al., 2017b; Sturtevant et al., 2015). These results highlight the need to integrate temporal factors and the legacy of historical disturbances into models of defoliation dynamics and forest management strategies. By appreciating the impact of previous conditions, managers can more effectively predict the severity of outbreaks, prioritize intervention strategies, and work towards preserving the ecological integrity of forest ecosystems over time. Such a cumulative effect aligns with previous research indicating that repeated defoliation episodes gradually erode a tree's vigor, increasing subsequent infestation risks (Régnière and Nealis, 2007; Sturtevant et al., 2015). By capturing these feedback loops, the ACAR model thus provides a more realistic representation of defoliation trajectories in these vulnerable forest stands.

4.4. Advancements in management strategies

Although our findings support prior research advocating for differentiated management strategies in boreal forests (Park et al., 2014; MacLean, 2016; James et al., 2011; Hennigar and MacLean, 2010; Venier and Holmes, 2010; Chavardès et al., 2021), they also provide significant advancements for managing SBW outbreaks in these ecosystems. Modeling using the ACAR framework, which accounts for both cumulative and autoregressive effects of defoliation, followed by clustering, emerges as a valuable tool for environmental segmentation to inform targeted strategies, identify complex and transitional zones, and optimize resource allocation. Homogeneous clusters, such as clusters 4 and 5 identified in our analysis, enable the recognition of specific climatic zones where long-term management strategies can be effectively planned. By tailoring management approaches to the unique characteristics of each cluster, resource allocation can be optimized, prioritizing interventions in the most vulnerable or unstable areas. The heterogeneous outcomes highlight the role of local environmental conditions — such as topography, microclimate, and more — in shaping SBW outbreak dynamics. Consequently, they underscore the need for nuanced, site-specific modeling approaches rather than generic prescriptions, ensuring that forest management strategies can be better aligned with the particular climatic and ecological contexts of each landscape.

5. Conclusion

This study enhances our understanding of the non-linear and region-specific dynamics associated with SBW outbreaks. The clustering analysis of landscape units highlights the critical importance of accounting for local heterogeneity: certain clusters reveal distinct opportunities for targeted interventions, whereas others exhibit more complex, overlapping trajectories that warrant further investigation. By assimilating these insights, it becomes apparent that adaptive and differentiated management strategies, tailored to the specific conditions of each cluster, are vital to mitigating both the ecological and economic consequences of SBW outbreaks.

Looking ahead, spatially explicit and temporally sensitive modeling approaches can refine predictions regarding the timing and location of

outbreaks. Incorporating spatial dependencies into these models will allow us to better capture the influence of forest composition, geographic features, and climate on both the initiation and propagation of outbreaks. In particular, extending the ACAR framework to account for spatial autocorrelation could improve predictive accuracy and provide more realistic representations of cross-boundary spread processes such as larval dispersal and host connectivity.

Beyond reaffirming the documented influence of climate, this study advances the field in three key ways. First, it demonstrates that SBW responses to seasonal temperature gradients are non-linear, revealing thresholds that mark tipping ranges for outbreak intensification or decline. Second, it explicitly captures epidemic legacy effects by embedding autoregressive terms in an ordinal framework, thereby quantifying the ecological memory of each landscape unit. Third, it introduces a novel clustering approach based on bidirectional AIC distance, which groups landscapes according to the functional similarity of their outbreak dynamics rather than static abiotic descriptors.

Together, these innovations move beyond descriptive correlations and provide an operational framework for forest management. By segmenting the boreal forest into clusters with distinct outbreak trajectories, the approach enables managers to tailor interventions to zones of high vulnerability, anticipate threshold crossings, and avoid one-size-fits-all prescriptions. While host composition and extreme climatic events such as spring warm spells were not explicitly modeled, integrating these factors represents a promising avenue for future research. Ultimately, this framework contributes both conceptually and practically to adapting spruce budworm management strategies to the reality of climate-driven disturbance dynamics.

CRediT authorship contribution statement

Olaloudé Judicaël Franck Osse: Writing – original draft, Visualization, Software, Formal analysis, Data curation, Conceptualization. **Philippe Marchand:** Writing – review & editing, Supervision, Software, Funding acquisition, Conceptualization. **Miguel Montoro Girona:** Writing – review & editing, Supervision, Funding acquisition, Conceptualization.

Availability of data and material

The datasets and R scripts used and/or analyzed during the current study are available from the corresponding author upon request.

Funding

PM and MMG obtained funding from the Natural Sciences and Engineering Research Council of Canada (NSERC) Alliance and the Québec Ministry of Natural Resources and Forests (MRNF) to understand the dynamics of spruce budworm (ALLRP 558267-20). MMG obtained additional funding from an NSERC Discovery grant to reconstruct the regime of natural disturbances in forest ecosystems (RGPIN-2022-05423).

Declaration of competing interest

The authors declare that they have no known competing financial interests or personal relationships that could have appeared to influence the work reported in this paper.

Data availability

Data will be made available on request.

References

Abarca, M., Lill, J.T., 2015. Warming affects hatching time and early season survival of eastern tent caterpillars. Oecologia 179, 901–912.
Abdi, H., Williams, L.J., 2010. Tukey's honestly significant difference (HSD) test. Encycl. Res. Des. 3 (1), 1–5.
Agresti, A., Kateri, M., 2011. Categorical data analysis. In: International Encyclopedia of Statistical Science. Springer, pp. 206–208.
Anderson, D.P., Sturtevant, B.R., 2011. Pattern analysis of eastern spruce budworm Choristoneura fumiferana dispersal. Ecography 34 (3), 488–497.
Balducci, L., Fierravanti, A., Rossi, S., Delzon, S., De Grandpré, L., Kneeshaw, D.D., Deslauriers, A., 2020. The paradox of defoliation: declining tree water status with increasing soil water content. Agricult. Forest. Meterol. 290, 108025.
Beckwith, R.C., Burnell, D.G., 1982. Spring larval dispersal of the western spruce budworm (Lepidoptera: Tortricidae) in north-central Washington. Environ. Èntomol. 11 (4), 828–832.
Bellemin-Noël, B., Bourassa, S., Despland, E., De Grandpré, L., Pureswaran, D.S., 2021. Improved performance of the eastern spruce budworm on black spruce as warming temperatures disrupt phenological defences. Global Change Biol. 27 (14), 3358–3366.
Berguet, C., Martin, M., Arseneault, D., Morin, H., 2021. Spatiotemporal dynamics of 20th-century Spruce Budworm outbreaks in eastern Canada: Three distinct patterns of outbreak severity. Front. Ecol. Evol. 8, 544088.
Black, E.N., Pureswaran, D.S., Marshall, K.E., 2024. Temperature fluctuations influence predictions of landscape-scale patterns of spruce budworm defoliation. BioRxiv 2024-2008.
Bouchard, M., Auger, I., 2014. Influence of environmental factors and spatio-temporal covariates during the initial development of a spruce budworm outbreak. Landsc. Ecol. 29 (1), 111–126.
Bouchard, M., Régnière, J., Therrien, P., 2018. Bottom-up factors contribute to large-scale synchrony in spruce budworm populations. Can. J. Forest Res. 48 (3), 277–284.
Boulanger, Y., Arseneault, D., 2004. Spruce budworm outbreaks in eastern Quebec over the last 450 years. Can. J. Forest Res. 34 (5), 1035–1043.
Brockerhoff, E.G., Barbaro, L., Castagneyrol, B., Forrester, D.I., Gardiner, B., González-Olabarria, J.R., Lyver, P.O., Meurisse, N., Oxbrough, A., Taki, H., et al., 2017. Forest biodiversity, ecosystem functioning and the provision of ecosystem services.
Bürkner, P.-C., Vuorre, M., 2019. Ordinal regression models in psychology: A tutorial. Adv. Methods Pr. Psychol. Sci. 2 (1), 77–101.
Burnham, K.P., Anderson, D.R., 2002. Model Selection and Multimodel Inference: A Practical Information-Theoretic Approach. Springer.
Candau, J.-N., Fleming, R.A., Wang, X., 2018. Ecoregional patterns of spruce budworm—Wildfire interactions in central Canada's forests. Forests 9 (3), 137.
Chavardès, R.D., Gennaretti, F., Grondin, P., Cavard, X., Morin, H., Bergeron, Y., 2021. Role of mixed-species stands in attenuating the vulnerability of boreal forests to climate change and insect epidemics. Front. Plant Sci. 12, 658880.
Chen, C., Weiskittel, A., Bataineh, M., MacLean, D.A., 2017a. Evaluating the influence of varying levels of spruce budworm defoliation on annualized individual tree growth and mortality in Maine, USA and New Brunswick, Canada. Forest Ecol. Manag. 396, 184–194.
Chen, C., Weiskittel, A., Bataineh, M., MacLean, D.A., 2017b. Even low levels of spruce budworm defoliation affect mortality and ingrowth but net growth is more driven by competition. Can. J. Forest Res. 47 (11), 1546–1556. http://dx.doi.org/10.1139/cjfr-2017-0012, arXiv:https://doi.org/10.1139/cjfr-2017-0012.
Cooke, B.J., 2024. On the characterization of patterning in spruce budworm time-series data. Can. J. Forest Res..
Debaly, Z.M., Marchand, P., Girona, M.M., 2022. Autoregressive models for time series of random sums of positive variables: Application to tree growth as a function of climate and insect outbreak. Ecol. Model. 471, 110053. http://dx.doi.org/10.1016/j.ecolmodel.2022.110053, URL: https://www.sciencedirect.com/science/article/pii/S0304380022001636.
Delisle, J., Bernier-Cardou, M., Labrecque, A., 2022. Cold tolerance and winter survival of seasonally-acclimatised second-instar larvae of the spruce budworm, Choristoneura fumiferana. Ecol. Entomol. 47 (4), 553–565.
Deslauriers, A., Fournier, M.-P., Cartenì, F., Mackay, J., 2019. Phenological shifts in conifer species stressed by spruce budworm defoliation. Tree Physiol. 39 (4), 590–605.
Despland, E., Gundersen, M., Daoust, S.P., Mader, B.J., Delvas, N., Albert, P.J., Bauce, E., 2011. Taste receptor activity and feeding behaviour reveal mechanisms of white spruce natural resistance to eastern spruce budworm Choristoneura fumiferana. Physiol. Entomol. 36 (1), 39–46.
Doran, O., MacLean, D.A., Kershaw, J.A., 2017. Needle longevity of balsam fir is increased by defoliation by spruce budworm. Trees 31, 1933–1944.
Dudek, A., 2020. Silhouette index as clustering evaluation tool. In: Classification and Data Analysis: Theory and Applications 28. Springer, pp. 19–33.
Eickenscheidt, N., Augustin, N., Wellbrock, N., 2019. Spatio-temporal modelling of forest monitoring data: modelling German tree defoliation data collected between 1989 and 2015 for trend estimation and survey grid examination using GAMMs. IForest-Biogeosci. For. 12 (4), 338.

Eveleigh, E.S., Johns, R.C., 2014. Intratree variation in the seasonal distribution and mortality of spruce budworm (Lepidoptera: Tortricidae) from the peak to collapse of an outbreak. Ann. Entomol. Soc. Am. 107 (2), 435–444.

Fierravanti, A., Cocozza, C., Palombo, C., Rossi, S., Deslauriers, A., Tognetti, R., 2015. Environmental-mediated relationships between tree growth of black spruce and abundance of spruce budworm along a latitudinal transect in Quebec, Canada. Agricult. Forest. Meterol. 213, 53–63.

Fierravanti, A., Rossi, S., Kneeshaw, D., Grandpré, L.D., Deslauriers, A., 2019. Low non-structural carbon accumulation in spring reduces growth and increases mortality in conifers defoliated by Spruce Budworm. Front. For. Glob. Chang. http://dx.doi.org/10.3389/ffgc.2019.00015.

Flower, A., Gavin, D., Heyerdahl, E., Parsons, R., Cohn, G., 2014. Drought-triggered western spruce budworm outbreaks in the interior Pacific northwest: a multi-century dendrochronological record. Forest Ecol. Manag. 324, 16–27.

Fortin, M., Lavoie, J.-F., Régnière, J., Saint-Amant, R., 2022. A web API for weather generation and pest development simulation in North America. Environ. Model. Softw. 157, 105476, URL: https://doi.org/10.1016/j.envsoft.2022.105476.

Frelich, L.E., Johnstone, J., Kuuluvainen, T., 2024. Boreal forests. In: Future Forests. Elsevier, pp. 221–242.

Gauthier, S., Kuuluvainen, T., Macdonald, S.E., Shorohova, E., Shvidenko, A., Bélisle, A.-C., Vaillancourt, M.-A., Leduc, A., Grosbois, G., Bergeron, Y., et al., 2023. Ecosystem management of the boreal forest in the era of global change. In: Boreal Forests in the Face of Climate Change: Sustainable Management. Springer, pp. 3–49.

Goodhue, J., Ervin, S., Hatheway, J.R., Ren, J., et al., 2017. Cockroaches' increasing metabolic rate with rising temperatures. J. Introd. Biol. Investig. 6 (1).

Gray, D.R., 2013. The influence of forest composition and climate on outbreak characteristics of the spruce budworm in eastern Canada. Can. J. Forest Res. 43 (12), 1181–1195.

Hanberry, B.B., 2022. Non-native plant associations with wildfire, tree removals, and deer in the eastern United States. Landsc. Online 1104–1104.

Hansen, M.C., Stehman, S.V., Potapov, P.V., 2010. Quantification of global gross forest cover loss. Proc. Natl. Acad. Sci. 107 (19), 8650–8655.

Hayes, M.B., Jiao, L., Tsao, T.-h., King, I., Jennings, M., Hou, C., 2015. High temperature slows down growth in tobacco hornworms (Manduca sexta larvae) under food restriction. Insect Sci. 22 (3), 424–430.

Hennigar, C.R., MacLean, D.A., 2010. Spruce budworm and management effects on forest and wood product carbon for an intensively managed forest. Can. J. Forest Res. 40 (9), 1736–1750.

Hilborn, R., Mangel, M., 1997. The Ecological Detective: Confronting Models with Data. Vol. 28, Princeton University Press.

Houndode, D.J., Krause, C., Morin, H., 2021. Predicting balsam fir mortality in boreal stands affected by spruce budworm. Forest Ecol. Manag. 496, 119408. http://dx.doi.org/10.1016/J.FORECO.2021.119408.

Howe, M., Hart, S.J., Trowbridge, A.M., 2024. Budworms, beetles and wildfire: Disturbance interactions influence the likelihood of insect-caused disturbances at a subcontinental scale. J. Ecol. 112 (11), 2567–2584.

James, P.M., Fortin, M.-J., Sturtevant, B., Fall, A., Kneeshaw, D., 2011. Modelling spatial interactions among fire, spruce budworm, and logging in the boreal forest. Ecosystems 14, 60–75.

Jennings, D.T., Houseweart, M.W., Dimond, J.B., 1983. Dispersal losses of early-instar spruce budworm (Lepidoptera: Tortricidae) larvae in strip clearcut and dense spruce-fir forests of Maine. Environ. Èntomol. 12 (6), 1787–1792.

Jolly, W.M., Cochrane, M.A., Freeborn, P.H., Holden, Z.A., Brown, T.J., Williamson, G.J., Bowman, D.M., 2015. Climate-induced variations in global wildfire danger from 1979 to 2013. Nat. Commun. 6 (1), 7537.

Kassambara, A., Mundt, F., 2017. Package 'factoextra'. Extr. Vis. Results Multivar. Data Anal. 76 (2).

Kneeshaw, D.D., De Grandpré, L., D'Orangeville, L., Marchand, M., Moisan-Perrier, J., Robert, L.-E., Bouchard, M., 2022. Forest structure and composition diverge following harvesting compared to a spruce budworm Choristoneura fumiferana (Clem.) outbreak. Front. For. Glob. Chang. 5, 680262.

Lemay, A., Barrette, J., Krause, C., 2022. Balsam fir (Abies balsamea (L.) Mill.) wood quality after defoliation by Spruce Budworm (Choristoneura fumiferana Clem.) in the Boreal Forest of Quebec, Canada. Forests http://dx.doi.org/10.3390/f13111926.

Li, M., MacLean, D.A., Hennigar, C.R., Ogilvie, J., 2020. Previous year outbreak conditions and spring climate predict spruce budworm population changes in the following year. Forest Ecol. Manag. 458, 117737.

MacLean, D.A., 2016. Impacts of insect outbreaks on tree mortality, productivity, and stand development. Can. Èntomol. 148 (S1), S138–S159.

MacLean, D.A., Collier, J., MacKinnon, W.E., Porter, K.B., 2024. Defoliation level interacts with tree species and soil richness to determine volume increment reduction and recovery from simulated spruce budworm attack. Can. J. Forest Res. 54 (10), 1155–1169.

Maechler, M., Rousseeuw, P., Struyf, A., Hubert, M., Hornik, K., Studer, M., Roudier, P., Gonzalez, J., 2013. Package 'cluster'. Dosegljivo Na 980.

Moise, E.R., Lavigne, M.B., Johns, R.C., 2019. Density has more influence than drought on spruce budworm (Choristoneura fumiferana) performance under outbreak conditions. Forest Ecol. Manag. 433, 170–175.

Moise, E.R., Warren, J., Bowden, J.J., 2024. Impacts of winter warming events on spruce budworm: the importance of timing. J. Insect Sci. 24 (2), 17.

MRNF, 2022. Ministère des ressources naturelles et des forêts. Données sur les perturbations naturelles - insecte : Tordeuse des bourgeons de l'épinette. URL: https://www.donneesquebec.ca/recherche/dataset/donnees-sur-les-perturbations-naturelles-insecte-tordeuse-des-bourgeons-de-lepinette. [Online; Accessed 6 November 2024].

Murtagh, F., Legendre, P., 2014. Ward's hierarchical agglomerative clustering method: which algorithms implement ward's criterion? J. Classification 31, 274–295.

Navarro, L., Morin, H., Bergeron, Y., Girona, M.M., 2018. Changes in spatiotemporal patterns of 20th century spruce budworm outbreaks in eastern Canadian boreal forests. Front. Plant Sci. 9, 1905.

Nealis, V., Régnière, J., 2004. Insect host relationships influencing disturbance by the spruce budworm in a boreal mixedwood forest. Can. J. Forest Res. 34 (9), 1870–1882.

Nealis, V., Régnière, J., 2021. Ecology of outbreak populations of the western spruce budworm. Ecosphere 12 (7), e03667.

O'Connell, B.P., Wiley, E., 2024. Heatwaves do not limit recovery following defoliation but alter leaf drought tolerance traits. Plant Cell Environ. 47 (2), 482–496.

Osse, O.J.F., Debaly, Z.M., Marchandb, P., Girona, M.M., 2023. Adjacent-category models for ordinal time series and their application to climate-dependent spruce budworm defoliation dynamics. arXiv preprint arXiv:2309.04688.

Overpeck, J.T., Rind, D., Goldberg, R., 1990. Climate-induced changes in forest disturbance and vegetation. Nature 343 (6253), 51–53.

Paixao, C., Krause, C., Morin, H., Achim, A., 2019. Wood quality of black spruce and balsam fir trees defoliated by spruce budworm: A case study in the boreal forest of Quebec, Canada. Forest Ecol. Manag. 437, 201–210.

Pan, Y., Birdsey, R.A., Fang, J., Houghton, R., Kauppi, P.E., Kurz, W.A., Phillips, O.L., Shvidenko, A., Lewis, S.L., Canadell, J.G., et al., 2011. A large and persistent carbon sink in the world's forests. Science 333 (6045), 988–993.

Park, A., Puettmann, K., Wilson, E., Messier, C., Kames, S., Dhar, A., 2014. Can boreal and temperate forest management be adapted to the uncertainties of 21st century climate change? Crit. Rev. Plant Sci. 33 (4), 251–285.

Pebesma, E., 2018. Simple features for r: Standardized support for spatial vector data. R J. 10 (1).

Portalier, S., Candau, J.-N., Lutscher, F., 2024. Larval mortality from phenological mismatch can affect outbreak frequency and severity of a boreal forest defoliator. Ecol. Model. 493, 110724.

Pureswaran, D.S., De Grandpré, L., Paré, D., Taylor, A., Barrette, M., Morin, H., Régnière, J., Kneeshaw, D.D., 2015. Climate-induced changes in host tree–insect phenology may drive ecological state-shift in boreal forests. Ecology 96 (6), 1480–1491.

Pureswaran, D.S., Neau, M., Marchand, M., De Grandpré, L., Kneeshaw, D., 2019. Phenological synchrony between eastern spruce budworm and its host trees increases with warmer temperatures in the boreal forest. Ecol. Evol. 9 (1), 576–586.

R Core Team, 2024. R: A Language and Environment for Statistical Computing. R Foundation for Statistical Computing, Vienna, Austria, URL: https://www.R-project.org/.

Ramachandran, R., 1987. Influence of host-plants on the wind dispersal and the survival of an Australian geometrid caterpillar. Èntomol. Exp. Appl. 44 (3), 289–294.

Régnière, J., Nealis, V., 2007. Ecological mechanisms of population change during outbreaks of the spruce budworm. Ecol. Entomol. 32 (5), 461–477.

Régnière, J., Nealis, V.G., 2019. Influence of temperature on historic and future population fitness of the western spruce budworm, Choristoneura occidentalis. Int. J. Pest Manag. 65 (3), 228–243.

Régnière, J., St-Amant, R., Duval, P., 2012. Predicting insect distributions under climate change from physiological responses: spruce budworm as an example. Biol. Invasions 14, 1571–1586.

Reichenbach, N.G., Stairs, G.R., 1985. Bioenergetics of the western spruce budworm (Lepidoptera: Tortricidae) with comments on endotherm and ectotherm population energetics. Can. J. Zool. 63 (6), 1330–1338.

Ren, P., Néron, V., Rossi, S., Liang, E., Bouchard, M., Deslauriers, A., 2020. Warming counteracts defoliation-induced mismatch by increasing herbivore-plant phenological synchrony. Global Change Biol. 26 (4), 2072–2080.

Rose, A., Blais, J., 1954. A relation between april and may temperatures and Spruce Budworm Larval Emergence1. Can. Èntomol. 86 (4), 174–177.

Royama, T., 1984. Population dynamics of the spruce budworm Choristoneura fumiferana. Ecol. Monograph. 54 (4), 429–462.

Saucier, J.-P., Gosselin, J., Morneau, C., Grondin, P., 2010. Utilisation de la classification de la végétation dans l'aménagement forestier au Québec. Rev. For. FranCovcaise 62 (3–4), 428–438.

Seidl, R., Fortin, M.-J., Honkaniemi, J., Lucash, M., 2023. Modeling natural disturbances in boreal forests. In: Boreal Forests in the Face of Climate Change: Sustainable Management. Springer, pp. 591–612.

Seidl, R., Honkaniemi, J., Aakala, T., Aleinikov, A., Angelstam, P., Bouchard, M., Boulanger, Y., Burton, P.J., De Grandpré, L., Gauthier, S., et al., 2020. Globally consistent climate sensitivity of natural disturbances across boreal and temperate forest ecosystems. Ecography 43 (7), 967–978.

Seidl, R., Thom, D., Kautz, M., Martin-Benito, D., Peltoniemi, M., Vacchiano, G., Wild, J., Ascoli, D., Petr, M., Honkaniemi, J., et al., 2017. Forest disturbances under climate change. Nat. Clim. Chang. 7 (6), 395–402.

Sidhu, H., Kidd, K., Emilson, E., Stastny, M., Venier, L., Kielstra, B., McCarter, C., 2024. Increasing spruce budworm defoliation increases catchment discharge in conifer forests. Sci. Total Environ. 912, 168561.

Stahle, L., Wold, S., et al., 1989. Analysis of variance (ANOVA). Chemometr. Intell. Lab. Syst. 6 (4), 259–272.

Sturtevant, B.R., Cooke, B.J., Kneeshaw, D.D., MacLean, D.A., 2015. Modeling insect disturbance across forested landscapes: insights from the spruce budworm. In: Simulation Modeling of Forest Landscape Disturbances. Springer, pp. 93–134.

Subedi, A., Marchand, P., Bergeron, Y., Morin, H., Girona, M.M., 2023. Climatic conditions modulate the effect of spruce budworm outbreaks on black spruce growth. Agricult. Forest. Meterol. 339, 109548.

Thom, D., 2023. Natural disturbances as drivers of tipping points in forest ecosystems under climate change–implications for adaptive management. Forestry 96 (3), 305–315.

Tramblay, Y., Koutroulis, A., Samaniego, L., Vicente-Serrano, S.M., Volaire, F., Boone, A., Le Page, M., Llasat, M.C., Albergel, C., Burak, S., et al., 2020. Challenges for drought assessment in the Mediterranean region under future climate scenarios. Earth-Sci. Rev. 210, 103348.

Venier, L., Holmes, S., 2010. A review of the interaction between forest birds and eastern spruce budworm. Environ. Rev. 18 (NA), 191–207.

Volney, W.J.A., Fleming, R.A., 2000. Climate change and impacts of boreal forest insects. Agric. Ecosyst. Environ. 82 (1–3), 283–294.

Volney, W.J.A., Fleming, R.A., 2007. Spruce budworm (Choristoneura spp.) biotype reactions to forest and climate characteristics. Global Change Biol. 13 (8), 1630–1643.

Wang, Z., Zhou, Z., Wang, C., 2021. Defoliation-induced tree growth declines are jointly limited by carbon source and sink activities. Sci. Total Environ. 762, 143077.

Ward, S.F., Moon, R.D., Aukema, B.H., 2019. Implications of seasonal and annual heat accumulation for population dynamics of an invasive defoliator. Oecologia 190, 703–714.

Wickham, H., FranCovcois, R., Henry, L., Müller, K., 2023. Vaughan, d. dplyr: A grammar of data manipulation. R Packag. Version 1 (2).

Wood, S.N., 2017. Generalized Additive Models: An Introduction with R. Chapman and Hall/CRC.

Xu, W., Hisano, M., 2024. Spatial variation in boreal forest responses to global environmental change in western Canada. Agricult. Forest. Meterol. 355, 110140.

Zhang, B., MacLean, D.A., Johns, R.C., Eveleigh, E.S., 2018. Effects of hardwood content on balsam fir defoliation during the building phase of a spruce budworm outbreak. Forests 9 (9), 530.

Zhu, C., Zhang, X., Zhang, N., Hassan, M.A., Zhao, L., 2018. Assessing the defoliation of pine forests in a long time-series and spatiotemporal prediction of the defoliation using landsat data. Remote. Sens. 10 (3), http://dx.doi.org/10.3390/rs10030360, URL: https://www.mdpi.com/2072-4292/10/3/360.